Stand., **No. 36** (1971).
(31) B. Lindman and I. Lindqvist, *Chem. Scr.*, **1**, 195 (1971).
(32) G. Lindblom and B. Lindman in "Chemie, Physikalische Chemie und Anwendungstechnik der grenzflächenaktiven Stoffe", Vol. II, Carl Hanser Verlag, München, 1973, p 925.
(33) M. Eisenstadt and H. L. Friedman, *J. Chem. Phys.*, **44**, 1407 (1966).
(34) G. S. Kelly in "Water, a Comprehensive Treatise", Vol. 1, F. Franks, Ed., Plenum Press, New York, N.Y., 1972, p 363.
(35) P. Mukerjee, personal communication.
(36) I. D. Robb and R. Smith, *J. Chem. Soc., Faraday Trans. 1*, **70**, 287 (1974).
(37) E. G. Bloor and R. G. Kidd, *Can. J. Chem.*, **46**, 3425 (1968).
(38) R. H. Erlich and A. L. Popov, *J. Am. Chem. Soc.*, **93**, 5620 (1971).
(39) M. Herlem and A. I. Popov, *J. Am. Chem. Soc.*, **94**, 1431 (1972).
(40) M. S. Greenberg, R. L. Bodner, and A. I. Popov, *J. Phys. Chem.*, **77**, 2449 (1973).
(41) C. Deverell and R. E. Richards, *Mol. Phys.*, **10**, 551 (1966).
(42) O. Lutz, *Z. Naturforsch., Teil A*, **23**, 1202 (1968).

Bond Length Variations in Substituted Phosphoranes

James M. Howell

Contribution from the Department of Chemistry, Brooklyn College, City University of New York, Brooklyn, New York 11210. *Received November 11, 1974*

Abstract: Successive methylation or hydrogenation in the equatorial position of fluorophosphoranes produces strong decreases in the (P–F) axial overlap population obtained from extended Hückel calculations in agreement with experimental data. The trends are rationalized in terms of a repulsive interaction between the lone pairs of the axial fluorine atoms and the equatorial σ bonds. The structures of PF_5, PF_4CH_3, and $PF_3(CH_3)_2$ were optimized by the CNDO/2 method confirming the overlap population trends.

There has been a recent flush of interest in the molecular orbitals of phosphoranes at both the semiempirical[1] and ab initio levels.[2-5] Most of these studies have been directed at d orbital participation,[1,4] the pseudo-rotational process,[1-3] or conformational effects.[1,3,5] In this paper we examine another facet of phosphorane chemistry, bond length variation with substituent. It has been known[6] for some time that successive methylation of pentafluorophosphorane produces a steady effect wherein the P–F axial bonds, $(P-F)_{ax}$, increase in length faster than do the remaining P–F equatorial bonds, $(P-F)_{eq}$. See Table I.

These phenomena have been discussed in terms of electron pair repulsion theory by Gillespie[7] and qualitative molecular orbital theory by Bartell[8] and Gavin.[9] The present work represents the results of a series of extended Hückel[10] and CNDO/2[11] calculations wherein the structures PF_5, PF_4CH_3, $PF_3(CH_3)_2$, $PF_2(CH_3)_3$, PF_4H, PF_3H_2, and PF_2H_3 were examined and some optimization performed using CNDO/2 calculations.

Results and Discussion

Ideally the effect of substitution on bond length could be investigated through bond length optimization. However, the extended Hückel method does not generally yield satisfactory bond lengths upon optimization and our approach instead is to use Mulliken overlap populations as indicators of bond strength (and thus length) while actually holding the bond length constant for the various calculations.

We start by examining the effect of equatorial group electronegativity as shown in Figure 1 where we show the effect of successive methylation and hydrogenation in the equatorial positions of a PF_5.[12] The overlap populations show that the axial P–F bonds are weakened much more by substitution than are the remaining P–F equatorial bonds. Furthermore, it is interesting that the effect is approximately linear with the extent of substitution.

We may now inquire as to the source of the $(P-F)_{ax}$ overlap population decrease relative to the remaining $(P-F)_{eq}$ overlap populations. More specifically, we ask if the decrease is localized in the σ or π type interactions of the $(P-F)_{ax}$ bond. Furthermore, what is the role of d orbitals.

We start our inquiry by examining a model compound, $PL_2L_3^*$, wherein both L and L* resemble hydrogen atoms in that they bear only 1s orbitals and both the P–L and P–L* bond lengths are 1.44 Å. The L atoms occupy the axial positions and the L* the equatorial. Figure 2 shows the behavior of the $(P-L)_{ax}$ overlap population, a pure σ interaction, as a function of the decreasing electronegativity (i.e., the value of H_{ii}) of the equatorial L* atoms. (The value of H_{ii} for L is kept at −18.0 eV.) Without utilizing d orbitals there is a progressive decrease in the total overlap population for the $(P-L)_{ax}$ bond. Examining the contributions from the individual molecular orbitals shows that the weakening originates in the $2a_1'$ orbital. In order to understand this behavior we employ the interaction diagrams of Figure 3. In the middle of the diagram are the localized σ and σ^* $(P-L)_{ax}$ combinations, which are not affected (in the Hückel approximation) by the changes in the electronegativity of the equatorial L* atoms. When the L* atoms are of high electronegativity (left side of Figure 3) the $2a_1'$ orbital is derived primarily from the mixing of the L_3^* fragment and the axial σ combination. There is not much incorporation of the axial σ^* fragment. On the other hand, when the L_3^* is of higher energy (right side of Figure 3), both the axial σ and σ^* combinations mix into the $2a_1'$ orbital. Since the axial σ fragment is lower lying, it mixes in $(P-L)_{eq}$ antibonding while the higher lying σ^* combination mixes in bonding. There is a cancellation occurring in the contribution from the 3s orbital of the P and the $2a_1$ orbital is essentially nonbonding. Now, as the electronegativity of the L* atoms is decreased the energy of the L_3^* fragment is increased (as shown on the right of Figure 3). The energy gap between the σ^* combination and the L_3 fragment is lessened and the mixing of the $(P-L)_{ax}$ σ^* fragment into the $2a_1$ orbital increased. As a result the $2a_1'$ orbital becomes more decidedly $(P-L)_{ax}$ antibonding. On the other hand, the lowest occupied valence shell orbital, $1a_1'$, will have a more bonding $(P-L)_{ax}$ interaction as the L* electronegativity increases. This is simply because the $1a_1'$ orbital will become more and more the pure $(P-L)_{ax}$ σ combination of Figure 3.

Turning to the "with d" results displayed in Figure 2 we

Table I. The Experimentally Determined Structures and the Results of CNDO/2 Optimization for the Phosphoranes $PF_{5-n}R_n$ (R = $-CH_3$ and $-H$)

	$(P-F)_{ax}$		$(P-F)_{eq}$		P–R		$F_{ax}-P-R$		$F_{eq}-P-R$		
Molecule	Calcd	Obsd	Calcd	Obsd	Calcd	Obsd	Calcd	Obsd	Calcd	Obsd	Ref
PF_5	1.617	1.577	1.602	1.534							6
PF_4CH_3	1.628	1.612	1.609	1.543	1.682	1.780	97.0	91.8	120.4	122.2	6
$PF_3(CH_3)_2$	1.640	1.643	1.619	1.553	1.693	1.798	82.9	88.9	119.9	118.0	6
$PF_2(CH_3)_3$	1.650	1.685			1.709	1.813					15
PF_4H		1.594		1.550		1.360		90.		124.	14

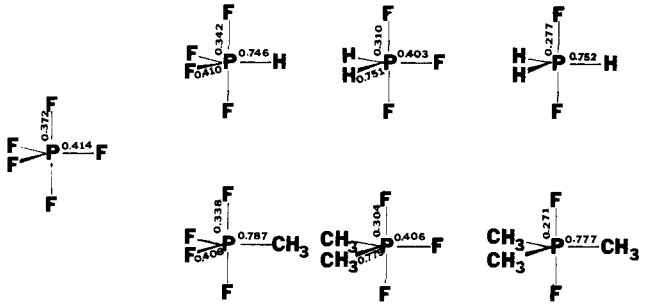

Figure 1. The overlap populations for some substituted phosphoranes obtained from extended Hückel calculations without d orbitals.

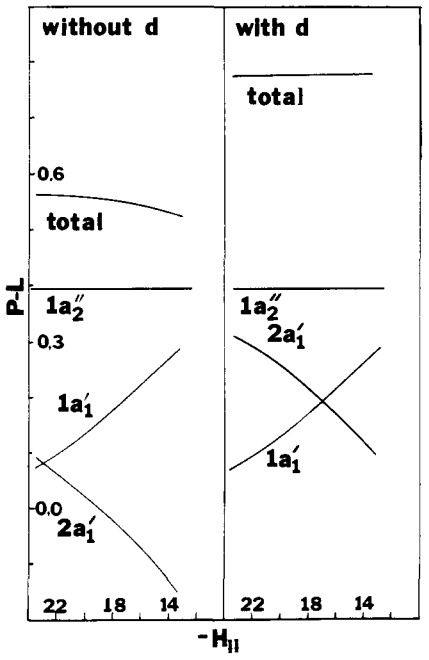

Figure 2. Contributions to the axial P–L overlap population for a model compound $PL_2L_3^*$ as a function of the electronegativity of the equatorial ligand L*.

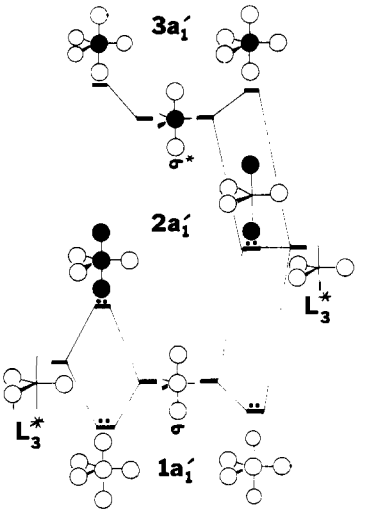

Figure 3. An interaction diagram for the molecule $PL_2L_3^*$ depicting the interaction of the axial σ and σ^* orbital combinations, in the middle, with two different types of equatorial ligands, L*. On the left the ligand L* is of high electronegativity while on the right L* is of moderate electronegativity.

see that the d orbitals actually cause the total σ-type overlap population for the $(P-L)_{ax}$ bond to increase slightly with decreasing L* electronegativity (for a change in the H_{ii} of 10 eV $(P-L)_{ax}$ changes by 0.0029). The d_{z^2} orbital participates strongly only in the $2a_1'$ orbital. (For a discussion of the extent of d orbital participation in the various phosphorane molecular orbitals, see ref 1 and 4.) This is easily understood in terms of the balance between the increasingly antibonding $1a_1'$ orbital and the increasingly bonding $2a_1'$ orbital. As L* becomes less electronegative the $2a_1'$ orbital becomes of higher energy thereby facilitating d orbital participation, counteracting the bond weakening trend. Thus the slope of the curve for the $2a_1'$ orbital in Figure 2 is more positive for the "with d" plot than for the "without d".

On the other hand, the $1a_1'$ orbital has very little d character (due to its nodal structure[1,4]) and thus the "with d" curve very closely resembles the "without d" case. The net balance is in favor of a strengthening of the $(P-L)_{ax}$ overlap population as L* becomes more electropositive. In sum it appears that any decrease in the σ $(P-L)_{ax}$ overlap population will be counterbalanced in proportion to the extent of d orbital participation.

To inspect the π system we again make use of a model structure: $PF_2L_3^*$. Of course, we now have π-like lone pairs on the axial fluorines. Again we vary the electronegativity of the equatorial L* 1s orbitals. Figure 4 displays the $(P-F)_{ax}$ overlap population, dissected into σ and π parts, and comparison with Figure 2 shows that the σ system of $PF_2L_3^*$ behaves similarly to that of the just discussed $PL_2L_3^*$: the weakening of the σ axial bond when decreasing the electronegativity of the L* atom calculated without d orbitals is strongly diminished or eliminated thru the inclusion of P 3d orbitals. Consequently, we do not pursue the analysis of the σ system any further.

The π-like lone pairs of the fluorines will interact with the phosphorane skeleton and the 3d orbitals of the P atom. First we consider the situation without d orbitals. The fluorine lone pairs may be symmetry adapted by taking the appropriate plus (e' symmetry), **1**, and minus (e''), **2**, combinations. Although the e'' combination will donate into the P 3d orbitals, it will not be able to interact, due to symmetry, with the σ phosphorane system. Thus we limit our discussion to the e' orbitals. The pertinent interactions for one member of the degenerate e' set of orbitals are displayed in

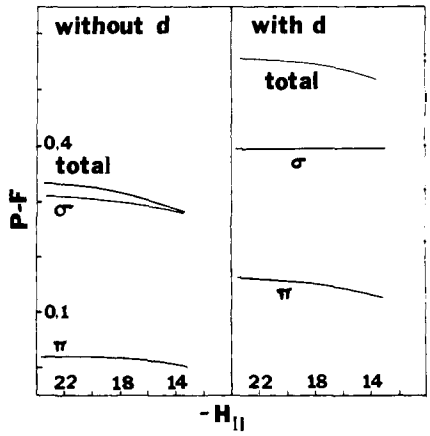

Figure 4. Contributions from the σ and π type orbitals to the axial P-F overlap population for the model compound PF_2L_3*, as a function of electronegativity of the equatorial ligand L*.

1 2

Figure 5. Again we show two interaction diagrams. On the right is the case where the L* atoms are of low electronegativity, modeling methyl groups or hydrogens, while on the left L* is of greater electronegativity thus providing the electron withdrawing ability of equatorial fluorine atoms.

In the center is the plus or bonding combination of the axial fluorine π orbitals (cf. **1**), the energy of which is not affected by changes in the electronegativity of the L* atoms. We next allow the F lone pairs to interact with the π-like combinations of the P-L σ equatorial bonds, forming a bonding, 1e′, and an antibonding, 2e′, combination, both of which will be occupied. There will be a substantial antibonding contribution to the $(P-F)_{ax}$ overlap population originating in the 2e′ orbitals. In the case of low L* electronegativity there are two factors which enhance the axial bond weakening interaction: (1) the PL_3* π-like σ bonding combination is of higher energy and thus mixes more strongly with the fluorine lone pairs; (2) there is a greater concentration of electron density on the P atom in the PL_3* fragment when L* is of low electronegativity.

Due to symmetry restrictions the role of d orbitals in the e′ orbitals is limited to the $d_{x^2-y^2}$ and d_{xy} orbitals lying in the equatorial plane. Further both the $d_{x^2-y^2}$ and d_{xy} orbital have zero overlap with the lone pairs of the axial fluorines. In order to account for the accelerated decrease in the π-type $(P-F)_{ax}$ overlap population, shown in Figure 4, when P 3d orbitals are included we again use the idea that the repulsive interaction between the P and F atoms within the 2e′ orbitals is proportional to the occupancy of the 3p orbital of the P atom; any occupancy of the $d_{x^2-y^2}$ or d_{xy} orbitals, which do not overlap with the atomic orbitals of the fluorine atoms, in the 2e′ orbitals will lessen the 3p occupancy thereby decreasing the antibonding interaction. Perhaps contrary to expectations, the 3d coefficient in the 2e′ orbital is greater in the case of a highly electronegative substituent, L*. For instance, with L* at −15.6 eV the 3d coefficient within the 2e′ orbital is 0.0393 while with the L* at −19.6 eV it is 0.0571. Equatorial substituents of low electronegativity will thus have little d orbital participation and consequently greater repulsive interaction between the P 3p orbital of the equatorial σ system and the axial fluorine lone pairs.

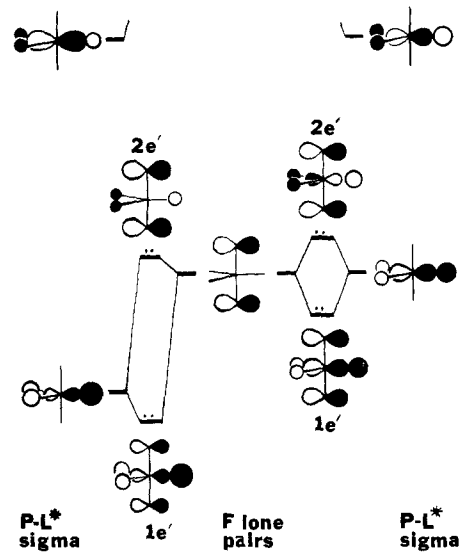

Figure 5. An interaction diagram schematically depicting the interaction of the axial fluorine π-like lone pairs (center) with the two different sets of π-like combinations of the equatorial σ bonds. On the left the ligand L* is of high electronegativity while on the right L* is of moderate electronegativity.

In locating the source of decrease in the $(P-F)_{ax}$ overlap population it appears that, without d orbitals, the effect is almost equally divided between the σ- and π-like interactions. However, as the d orbital participation is allowed the axial bond weakening becomes localized in the axial π system. It is hard to judge the situation in the actual molecule but surely the 3d orbitals must play some role therein. It seems likely that the π manifold effects are the more important.[13] This interpretation then dovetails nicely with the analysis of rotational barriers provided in ref 1.

A further exploration was carried out by optimizing the structure of PF_5, PF_4CH_3, $PF_3(CH_3)_2$, and $PF_2(CH_3)_3$ using a modified CNDO/2 program. The results are also given in Table I. As expected we see that methylation produces notable lengthening of the P-F axial bonds, while the equatorial bonds are lengthened to a lesser extent. The microwave structure[14] of PF_4H shown in Table I does not seem to fit the trend, the axial and equatorial bonds undergoing about the same lengthening upon hydrogenation. Whether this is a real distinction or not is uncertain since the reported[14] errors are fairly large especially in the $(P-F)_{ax}$ length, ±0.03.

Acknowledgment. The work was supported in part by a Faculty Research Award from the City University of New York. A generous grant of computer time was received from the Central Computer Facility of the City University of New York.

References and Notes

(1) R. Hoffmann, J. M. Howell, and E. L. Muetterties, *J. Am. Chem. Soc.*, **94**, 3047 (1972), and references therein.
(2) A. Rauk, L. C. Allen, and K. Mislow, *J. Am. Chem. Soc.*, **94**, 3035 (1972).
(3) A. Strich and A. Veillard, *J. Am. Chem. Soc.*, **95**, 5574 (1973).
(4) J. M. Howell, J. R. Van Wazer, and A. R. Rossi, *Inorg. Chem.*, **13**, 1747 (1974).
(5) J. M. Howell, *Chem. Phys. Lett.*, **25**, 51 (1974).
(6) L. S. Bartell and K. W. Hansen, *Inorg. Chem.*, **4**, 1775 (1965).
(7) R. J. Gillespie, *Inorg. Chem.*, **5**, 1634 (1966).
(8) L. S. Bartell, *Inorg. Chem.*, **5**, 1635 (1966).
(9) R. M. Gavin, *J. Chem. Educ.*, **46**, 413 (1969).
(10) R. Hoffmann, *J. Chem. Phys.*, **39**, 1397 (1963).
(11) J. A. Pople and D. L. Beveridge, "Approximate Molecular Orbital Theory", McGraw-Hill, New York, N.Y., 1970.
(12) The results shown were obtained by an extended Huckel program using P-F = 1.55 Å, P-H = 1.44 Å, P-C = 1.78 Å, C-H = 1.09 Å. Idealized

bond angles were used and Hoffmann's parameters (ref 10) were used for H, C, and F (H exponent = 1.3). Phosphorus parameters were H_{ii}: 3s −18.6 eV, 3p −14.0 eV, and an exponent of 1.6. Similar calculations were performed using 3d orbitals at −6.0 eV with an exponent of 1.4.

(13) This conclusion will, of course, depend somewhat on the choice of parameters.
(14) S. B. Pierce and C. D. Cornwell, *J. Chem. Phys.*, **48**, 2118 (1968).
(15) H. Yow and L. S. Bartell, *J. Mol. Struct.*, **15**, 209 (1973).

Photochemical Reductive Elimination of Oxygen, Hydrogen, and Hydrogen Chloride from Iridium Complexes

Gregory L. Geoffroy,[1a] George S. Hammond,[1b] and Harry B. Gray*[1c]

Contribution No. 5027 from the Arthur Amos Noyes Laboratory of Chemical Physics, California Institute of Technology, Pasadena, California 91125, the Department of Chemistry, University of California, Santa Cruz, California 95060, and the Department of Chemistry, The Pennsylvania State University, University Park, Pennsylvania 16802. *Received December 17, 1974*

Abstract: Ultraviolet irradiation of the H_2 and O_2 adducts of $[IrCl(CO)(Ph_3P)_2]$, $[IrI(CO)(Ph_3P)_2]$, $[Ir(2\text{-phos})_2]^+$, and $[Ir(2{=}phos)_2]^+$ (2-phos is 1,2-bis(diphenylphosphino)ethane and 2=phos is *cis*-1,2-bis(diphenylphosphino)ethylene) induces reductive elimination of molecular hydrogen and oxygen and regeneration of the square-planar complexes. The reactions occur in argon-purged solutions and in glasses at 77°K. Deoxygenation of $[O_2IrCl(CO)(Ph_3P)_2]$ can be made to go essentially to completion even in air-saturated solutions. Production of $O_2(^1\Delta_g)$ is not observed. Reductive elimination of HCl from $[H(Cl)IrCl(CO)(Ph_3P)_2]$ also occurs upon irradiation of argon-purged solutions. Electronic spectral data suggest that the lowest electronic excited state in each complex possesses iridium-to-phosphine charge-transfer character. It is believed that the photoelimination process is initiated in this CT excited state, but the detailed mechanism of formation of the diatomic product molecule (O_2, H_2, or HCl) is not known.

Oxidative-addition reactions of square-planar complexes of iridium(I) have been extensively investigated.[2-14] Vaska's complex, $[IrCl(CO)(Ph_3P)_2]$, and the related complexes $[IrI(CO)(Ph_3P)_2]$, $[Ir(2\text{-phos})_2]^+$,[15] and $[Ir(2{=}phos)_2]^+$,[15] among others, oxidatively add molecular oxygen and hydrogen, hydrogen chloride, and a large variety of other small molecules.[2,9] Of the O_2, H_2, and HCl adducts of these four complexes, however, only $[O_2IrCl(CO)(Ph_3P)_2]$ and $[H_2Ir(Cl)(CO)(Ph_3P)_2]$ undergo reductive-elimination reactions under mild conditions.[2,9,11] For example, $[O_2IrCl(CO)(Ph_3P)_2]$ loses oxygen when a solution of the complex is purged with an inert gas or when the solid is heated. By comparison, loss of oxygen does not occur from purged solutions of $[O_2Ir(2\text{-phos})_2]^+$ or when a solid sample of $[O_2Ir(2\text{-phos})_2]Cl$ is heated in vacuo at 110° for 24 hr.[9]

Very little is known about the photochemical behavior of the aforementioned adduct complexes. Vaska has briefly reported that orange crystals of $[O_2IrCl(CO)(Ph_3P)_2]$ are sensitive to light and change to green and then to blue-black on prolonged exposure and that the photoproduct probably contains triphenylphosphine oxide and an Ir(IV) complex.[5] In another communication, mention was made of an observation that the deoxygenation reaction of $[O_2IrCl(CO)(Ph_3P)_2]$ is photocatalyzed, but no details were given.[12] These observations prompted us to make an extensive study of the photochemistry of several adduct complexes of iridium. We find that thermally nonlabile adducts are labilized by ultraviolet irradiation of fluid solutions, under an inert gas purge, and of glasses at low temperature.

Experimental Section

Samples of $[IrCl(CO)(Ph_3P)_2]$ were obtained from Alfa Chemical Corporation and were used without further purification. $[Ir(2\text{-phos})_2]Cl$ and $[Ir(2{=}phos)_2]Cl$ were prepared by published methods.[9] $[IrI(CO)(PPh_3)_2]$ was provided by Professor J. G. Gordon, and $[O_2Co(2{=}phos)_2]ClO_4$ by Dr. V. Miskowski. Infrared and electronic absorption spectra of all five complexes were measured and found to be in excellent agreement with published data.[2,9,10] Tetramethylethylene (TME) was obtained from the Aldrich Chemical Co. All other chemicals used were reagent grade.

Preparation of Adducts. Adduct complexes were prepared by passing gaseous oxygen, hydrogen, or hydrogen chloride through solutions containing the four-coordinate iridium(I) complexes. Benzene solutions were employed for $[IrCl(CO)(Ph_3P)_2]$ and $[IrI(CO)(Ph_3P)_2]$, whereas adducts of $[Ir(2\text{-phos})_2]Cl$ and $[Ir(2{=}phos)_2]Cl$ were prepared in ethanol or acetonitrile. The reactions were considered to be complete when the characteristic visible absorption bands of the square-planar complexes disappeared. $[O_2IrCl(CO)(Ph_3P)_2]$ was isolated by concentrating the benzene solution, cooling in an ice bath under an atmosphere of oxygen, and filtering the resultant precipitate. $[O_2Ir(2\text{-phos})_2]Cl$ and $[O_2Ir(2{=}phos)_2]Cl$ were isolated by evaporation of the solvent followed by recrystallization from methylene chloride–diethyl ether. $[O_2IrI(CO)(Ph_3P)_2]$ was not isolated from benzene solution. The reactions with H_2 and HCl are much faster than the corresponding reactions with oxygen, and solid complexes were isolated in all cases.

Solution Irradiation. All irradiations were performed with a 150-W medium-pressure Hg lamp equipped with Corning glass 0-52 and 7-37 filters which pass only 366-nm light. The intensity of the lamp is ca. 10^{-7} einstein/min. The compound to be studied was dissolved in a suitable solvent (benzene for neutral complexes; ethanol or acetonitrile for ionic complexes) and placed in a 1-cm quartz spectrophotometer cell fitted with 3-in. neck and a serum cap. Solutions were purged by passing the appropriate gas (Ar, O_2, H_2) through the serum cap using standard syringe needle techniques.[16] The quartz cell was placed in a jacketed cell holder in front of the lamp and cooled with tap water. The cell was periodically removed and the absorption spectrum of the solution measured.

The relative rate of reductive-elimination of H_2 from $[H_2IrCl(CO)(PPh_3)_2]$ was determined by following the electronic absorption spectral changes of two 3-ml aliquots from a benzene so-